

RSC Advances



This is an *Accepted Manuscript*, which has been through the Royal Society of Chemistry peer review process and has been accepted for publication.

Accepted Manuscripts are published online shortly after acceptance, before technical editing, formatting and proof reading. Using this free service, authors can make their results available to the community, in citable form, before we publish the edited article. This *Accepted Manuscript* will be replaced by the edited, formatted and paginated article as soon as this is available.

You can find more information about *Accepted Manuscripts* in the [Information for Authors](#).

Please note that technical editing may introduce minor changes to the text and/or graphics, which may alter content. The journal's standard [Terms & Conditions](#) and the [Ethical guidelines](#) still apply. In no event shall the Royal Society of Chemistry be held responsible for any errors or omissions in this *Accepted Manuscript* or any consequences arising from the use of any information it contains.

Chemical Regeneration Mechanism of Fe-impregnated Chitosan Using Ferric Chloride

Jing Zhang^a, Nan Chen^{a,b,*}, Chuanping Feng^{a,b}, Miao Li^c, Long Lv^a, Qili Hu^a

^a Key Laboratory of Groundwater Cycle and Environment Evolution (China University of Geosciences (Beijing)), Ministry of Education, Beijing, 100083, China

^b School of Water Resources and Environment, China University of Geosciences (Beijing), Beijing, 100083, China

^c School of Environment, Tsinghua University, Beijing, 100084, China

*Correspondence: Nan Chen, School of Water Resources and Environment, China University of Geosciences (Beijing), Beijing 100083, China.

Tel: +86 10 82322281

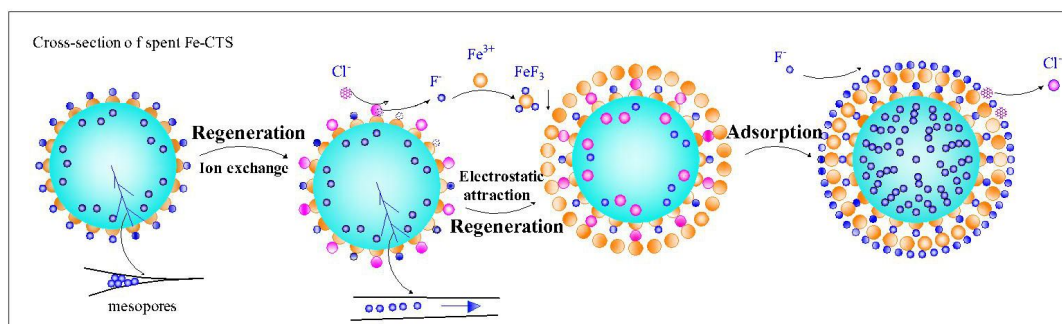
Fax: +86 10 82321081

E-mail address: chennan@cugb.edu.cn (N. Chen)

Highlights

- NaCl, FeCl₃ and CaCl₂ solutions were used as regenerants for Fe-impregnated chitosan (Fe-CTS), and best efficiency was obtained using FeCl₃.
- Negatively charged spent Fe-CTS turned to positively charged after regeneration by FeCl₃.
- Ion exchange and electrostatic attraction were regeneration and fluoride adsorption mechanisms.
- After seven regeneration/adsorption cycles, the adsorption capacity of FeCl₃ regenerated Fe-CTS was 74.04 mg/g without a significant loss in adsorption ability.

Graphical Abstract



Abstract: A process for the regeneration of spent Fe-impregnated chitosan (Fe-CTS) by continuous fluoride adsorption and chemical regeneration was described. Different concentrations of NaCl, FeCl₃ and CaCl₂ solutions were employed as regenerants. The regeneration efficiencies were valued using 100 mg/L fluoride adsorption on regenerated Fe-CTS. Results showed that the maximum adsorption capacity (q_e) of 14.44 mg/g was obtained when the Fe³⁺ regenerant concentration was 150 mg/L. Changes in F⁻ and Cl⁻ concentration were also measured. To examine the stability of regenerated Fe-CTS, Fe³⁺ leaching was observed in the fluoride solution after adsorption. Scanning electron microscopy with an electronic differential system and surface charge distribution were performed to elucidate the regeneration and adsorption mechanisms. Holes and cracks that emerged after regeneration accelerated the rate of internal diffusion. After regeneration, the FeCl₃ solution pH was less than pHPzc (4.92), indicating that FeCl₃ regenerated Fe-CTS (FeCl₃-Fe-CTS) was positively charged. The change in the concentration of fluoride was consistently greater than that of chloride, indicating that other mechanisms excepting ion-exchange, such as electrostatic attraction, contributed to fluoride adsorption. After seven regeneration/adsorption cycles, the total adsorption capacity of FeCl₃-Fe-CTS was found to be 74.04 mg/g without a significant loss in the adsorption ability.

Keywords: Regeneration; Fluoride adsorption; FeCl₃-Fe-CTS; Ion exchange; Electrostatic attraction

1. Introduction

High concentrations of fluoride in drinking water can contribute to various physical disorders, such as dental and skeletal fluorosis, brain damage, infertility and thyroid disorders [1]. The World Health Organization recommends a concentration of less than 1.5 mg/L [2]. Adsorption has been proven to be superior to other techniques for fluoride removal in terms of cost, ease of operation, simplicity of design and high removal efficiency [3]. However, the most serious disadvantage of adsorption is the generation of large quantities of spent adsorbents as solid wastes. It has been reported that 3404 tons per year of spent adsorbents are produced in an industrial complex in Korea. More than 70% of the total spent adsorbents are disposed of in landfills or incinerated [4]. Therefore, given the economic and environmental benefits, the regeneration of spent adsorbents is desirable.

Various methods have been developed to regenerate spent adsorbents, including chemical regeneration [5], heat regeneration [6], electrochemical regeneration [7], calcination [8] and microwave treatments [9]. Among the methods, chemical regeneration for chitosan-based adsorbents is a common method used for the removal of fluoride. The usually employed regenerants are sodium hydroxide solution [10], alkali-acid [11], alum solution [12] and ammonium chloride solution [13]. In our previous study, Fe-impregnated chitosan (Fe-CTS) was synthesized and employed for the adsorption of fluoride [14]. However, it was found that the fluoride adsorption capacity of Fe-CTS slightly varied with the pH values. Thus, neither the sodium hydroxide solution nor alkali-acid treatment could be used to regenerate Fe-CTS.

An important problem that has been neglected by researchers is the treatment of spent regenerants, which have high fluoride concentration that are discharged to wastewater. To solve this problem, ferric and calcium chloride solutions have been applied to regenerate spent Fe-CTS. In the previous study, it was found that fluoride adsorption on Fe-CTS occurred because of the ion exchange between chloride and fluoride moieties. Consequently, chloride has been used to try to exchange fluoride on Fe-CTS [14]. Moreover, to reduce secondary pollution and recycle fluoride, it was

expected that the fluoride exchanged by chloride would form a precipitate with ferric or calcium ions. In addition, because negatively charged adsorbents could attract positively charged ions [15], ferric and calcium ions were expected to be attracted on the surface of the negatively charged spent Fe-CTS so that positively charged regenerated Fe-CTS was obtained. In turn, positively charged regenerated Fe-CTS would attract negatively charged fluoride.

In this study, the effects of regeneration using ferric and calcium chloride solutions were measured. The effects of different concentrations of regenerants on fluoride adsorption onto regenerated Fe-CTS were investigated. A possible mechanism of regeneration by ferric chloride and fluoride adsorption were also investigated using a scanning electron microscopy (SEM) with an electronic differential system (EDS), fourier transform infrared spectroscopy (FTIR), X-ray diffraction (XRD), the nitrogen adsorption-desorption isotherm and surface charge distribution.

2. Materials and Methods

2.1 Materials

Spent Fe-CTS, obtained from the previous study of fluoride adsorption on Fe-CTS at an initial concentration of 100 mg/L fluoride and dosage of 5 g/L, was utilized for regeneration. NaF, $\text{FeCl}_3 \cdot 6\text{H}_2\text{O}$, CaCl_2 and NaCl were purchased from National Medicines (Shanghai, China). A fluoride stock solution (100 mg/L) was prepared by adding NaF (0.2210 g), which had been dried at 105 °C for 2 h, to deionized water (1000 mL). All chemicals used were of analytical reagent grade.

2.2 Regeneration of spent Fe-CTS

(1) For the $\text{FeCl}_3 \cdot 6\text{H}_2\text{O}$ treatment, spent Fe-CTS (0.25 g) was added to 50 mL FeCl_3 solution with Fe^{3+} concentrations of 30, 60, 90, 120 and 150 mg/L (The corresponding Cl^- concentrations were 57.05, 114.11, 171.16, 228.21, 285.27 mg/L, respectively) in 200 mL conical flasks. The conical flasks were shaken at 100 rpm at 30 °C for 45 min. Liquid samples were taken after filtration through a 0.45 μm cellulose acetate filter. The FeCl_3 regenerated Fe-CTS (FeCl_3 -Fe-CTS) was dried at 50 °C for 12 h. The fluoride concentration was measured.

(2) For the CaCl_2 treatment, spent Fe-CTS (0.25 g) was added to 50 mL CaCl_2 solution with Ca^{2+} concentrations of 30, 60, 90, 150 and 300 mg/L (The corresponding Cl^- concentrations were 53.25, 106.50, 159.95, 266.25, 532.50 mg/L, respectively) in 200 mL conical flasks. The CaCl_2 regenerated Fe-CTS (CaCl_2 -Fe-CTS) was obtained, and the fluoride concentration was measured.

(3) Considering the effect of regeneration by Cl^- , control experiments were conducted by adding spent Fe-CTS (0.25 g) to 50 mL NaCl solution (The corresponding Cl^- concentrations were 57.05, 114.11, 171.16, 228.21, 285.27, 532.50 mg/L, respectively) with equal concentrations of Cl^- in FeCl_3 and CaCl_2 solutions. NaCl regenerated Fe-CTS (NaCl-Fe-CTS) was obtained, and the fluoride concentration was measured.

2.3 Fluoride adsorption on regenerated Fe-CTS

To investigate the effect of the target chemical regenerants, 0.25 g of regenerated adsorbents was added into 200 mL conical flasks containing 50 mL of 100 mg/L fluoride solution. The conical flasks were shaken at 150 rpm at 30 °C for 6 h, under the same conditions as those of the previous study. Liquid samples were taken after filtration through a 0.45 μm cellulose acetate filter. Then, the concentration of F^- , Cl^- and Fe^{3+} or Ca^{2+} ions was measured.

The adsorption capacity (q_e , mg/g) is calculated as follows [16]:

$$q_e = (C_0 - C_e) \cdot V / W \quad (1)$$

where C_0 and C_e are the initial and equilibrium fluoride concentrations (mg/L), respectively; V is the total solution volume (L); and W is the mass of adsorbent (g).

The spent Fe-CTS were regenerated using 150 mg/L Fe^{3+} solution. Seven adsorption and regenerated cycles were conducted using 100 mg/L fluoride. Control experiments using spent Fe-CTS and a fluoride concentration of 100 mg/L were also performed for seven cycles.

2.4 Analytical methods

Fluoride concentration was measured using a fluoride ion selective electrode (F2021, DKK-TOA, Japan) [17]. The concentration of Fe^{3+} and Ca^{2+} ions was measured by

atomic absorption spectrometry (AAS 4001, Perkin-Elmer, USA) [18], and the concentration of Cl^- ions was measured by ion chromatography (ICS900, Dionex, USA) [19]. Surface morphological analysis, which was performed using a SEM (SSX-550, Shimadzu, Japan) fitted with an EDS, allowed the qualitative detection and localization of elements within the samples. FTIR spectroscopy were recorded (Vertex 70V, Bruker, Germany) with the attenuated total reflectance method from 4000 to 400 cm^{-1} at a resolution of 0.4 cm^{-1} . The crystalline structures were determined by X-ray diffraction (XRD) patterns obtained with a step time of 10 s and 2θ of 0.02° (D8 Advance, Bruker, Germany). The nitrogen adsorption-desorption isotherm and BJH (Barrett–Joyner–Halenda) pore size distribution of spent and regenerated Fe-CTS were determined using Brunauer–Emmett–Teller (BET) specific surface analysis device (JW-BK132F, JWGB, China).

3. Results and discussion

3.1 Desorption efficiency of regenerants

NaCl, FeCl_3 and CaCl_2 solution were employed to regenerate spent Fe-CTS. The results of desorption efficiency (Fig. 1) showed that all desorption efficiency measurements were less than 15%, which maybe because fluoride adsorption on the Fe-CTS was a chemisorption process. NaCl had little effect on the regeneration of Fe-CTS reflecting upon low efficiency at about 2%. The desorption efficiency of FeCl_3 and CaCl_2 rose from 2.01% and 3.09% to 12.00% and 11.48%, respectively, with increased Cl^- concentration. The difference between NaCl and FeCl_3 and CaCl_2

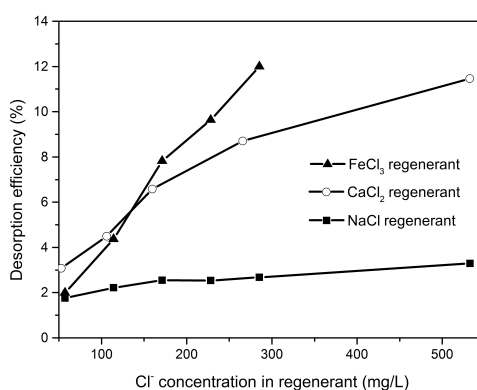


Fig. 1. Desorption efficiency of different regenerants (FeCl_3 , CaCl_2 , and NaCl).

may be attributed to the fact that Fe^{3+} and Ca^{2+} cations could react with F^- [20, 21] while Na^+ could coexist with F^- .

3.2 Fluoride adsorption on regenerated Fe-CTS

The performance of the treatment process was determined for Fe-CTS regenerated using a range of regenerant concentrations. The measured adsorption capacity as a function of NaCl, FeCl_3 and CaCl_2 showed that a maximum q_e of 14.44 mg/g, which was found to be close to the maximum of fresh Fe-CTS (14.99 mg/g), was reached when the Fe^{3+} concentration of the regenerant was 150 mg/L, as shown in Fig. 2.

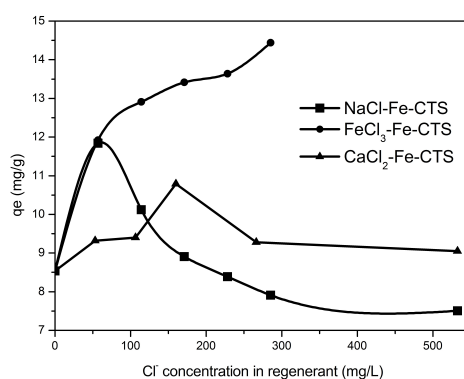


Fig.2. Fluoride adsorption on regenerated Fe-CTS.

Overall, the results confirmed that regeneration of the adsorbent was being achieved. In the absence of regeneration, the adsorption capacity was 8.54 mg/g. As the Cl^- concentration was increased, the fluoride adsorption capacity of FeCl_3 -Fe-CTS rose from 8.54 to 14.44 mg/g, while that of NaCl-Fe-CTS declined from 11.84 to 7.51 mg/g. At the same time, the CaCl_2 solution exhibited less regeneration efficiency for fluoride adsorption capacity. Comparatively, CaCl_2 displayed a positive effect on regeneration in response to the existence of Ca^{2+} . Xiang et al. [22] found that the existence of Ca^{2+} could enhance fluoride adsorption; however, adsorption capacity was not proportional to the amount of Ca^{2+} in the adsorbents, which was the same tendency as the results in the present study. The adsorption capacity increased slowly to a maximum Ca^{2+} concentration of 90 mg/L and then declined slowly. According to the pH of CaCl_2 and NaCl regenerant after regeneration (showed in Supplementary data Table S1), it is clear that pH of CaCl_2 and NaCl regenerant after regeneration showed the same trends with their adsorption capacity. This demonstrated that the decrease of adsorption capacity when the Ca^{2+} concentration was larger than 90 mg/L

and NaCl solution at high concentrations were due to the effect of electrostatic attraction. In addition, large amount of Cl^- was adsorbed when Cl^- concentration (228.21, 285.27 mg/L) were high in regenerant, which maybe made fluoride adsorption relatively difficult when fluoride concentration (100 mg/L) was far smaller than Cl^- concentration. The different effects among FeCl_3 , NaCl and CaCl_2 may result in part from the fact that the FeCl_3 solution was acidic while the NaCl and CaCl_2 solutions were neutral. It has been reported that using an acidic solution as a regenerant had an activating effect on chitosan-based adsorbents [11, 23]. This was also consistent with the result in the previous study that showed that fluoride adsorption capacity would decline slightly in an acidic environment [14]. Another reason has been reported [20], i.e. that multivalent cations were more strongly attracted to negatively charged adsorbents than positively charged adsorbents such that more fluoride adsorption sites emerged when Fe^{3+} and Ca^{2+} adsorbed onto the spent Fe-CTS.

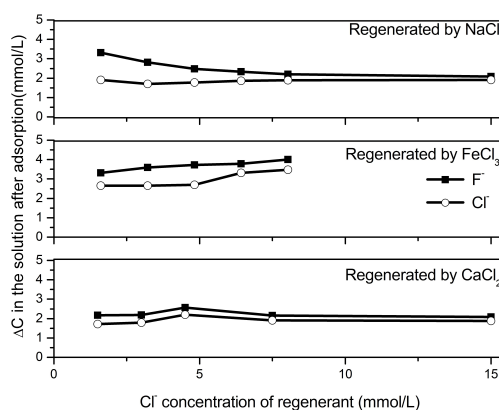


Fig.3. Change in concentration of F^- and Cl^- after adsorption.

To investigate the different regeneration results among the three regenerants and the relationship between fluoride ions and chloride ions, the change in F^- and Cl^- concentration in an aqueous solution after adsorption was measured. The three regenerants demonstrated three different tendencies, as shown in Fig. 3. A slight fluctuation was found in Cl^- concentration for NaCl-Fe-CTS with a slow decrease in F^- concentration. The most likely explanation for this finding was that chloride adsorption during generation resulted in a greater negative charge on the adsorbent surface. Generally, fluoride ion adsorption involves two steps: first, fluoride ions are

drawn to the adsorbent through electrostatic attraction; second, a chemical reaction occurs when the fluoride reached the surface of adsorbents. In our study, the negatively charged Fe-CTS repulsed the negatively charged fluoride ions. For FeCl₃-Fe-CTS, the change in the Cl⁻ concentration increased with increasing F⁻. A similar significant trend was evident for CaCl₂. The different tendencies maybe because, under acidic conditions, the chloride ions were easy to be exchanged. In addition, it should be noted that the change in chloride with FeCl₃-Fe-CTS was higher than that of the NaCl-Fe-CTS and CaCl₂-Fe-CTS. Considering the regenerative effect, FeCl₃-Fe-CTS was employed for further study.

3.3 Characterization of FeCl₃-Fe-CTS

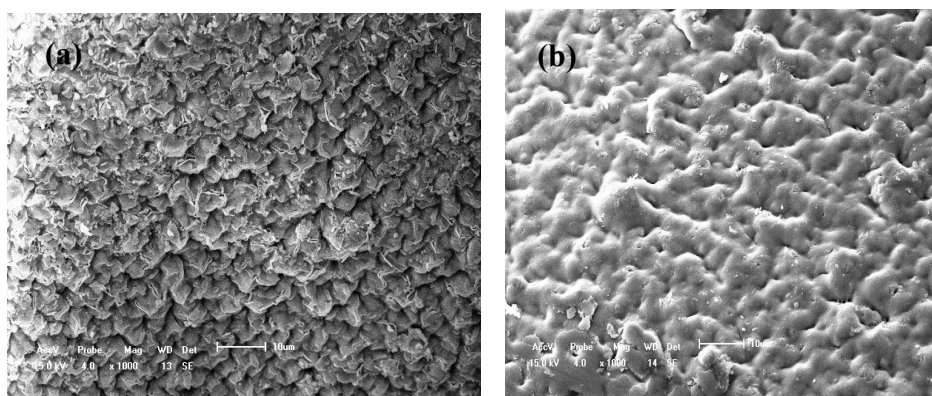


Fig. 4. SEM images of FeCl₃-Fe-CTS (a) before adsorption, (b) after adsorption for 6 h.

Fig. 4 showed the SEM images (1000 \times) of FeCl₃-Fe-CTS before and after fluoride adsorption. Different from spent Fe-CTS, which had a smooth surface and no sharp edges, the morphology of FeCl₃-Fe-CTS was much more similar to fresh Fe-CTS with an uneven surface structure. The cracks on the surface may be due to immersion in an acidic solution of ferric and dry in the oven. Comparatively, more irregularities on the surface have been reported to improve adsorption capacity [24]. In contrast, after adsorption, the adsorbent showed a very high degree of similarity to spent Fe-CTS; many holes were observed on the adsorbent surface.

Fig. 5 showed the nitrogen adsorption-desorption isotherms and pore-size distribution curve of Fe-CTS, NaCl-Fe-CTS, CaCl₂-Fe-CTS and FeCl₃-Fe-CTS. As seen, all the adsorbents exhibited a type IV isotherm according to IUPAC classification, which was associated with capillary condensation taking place in

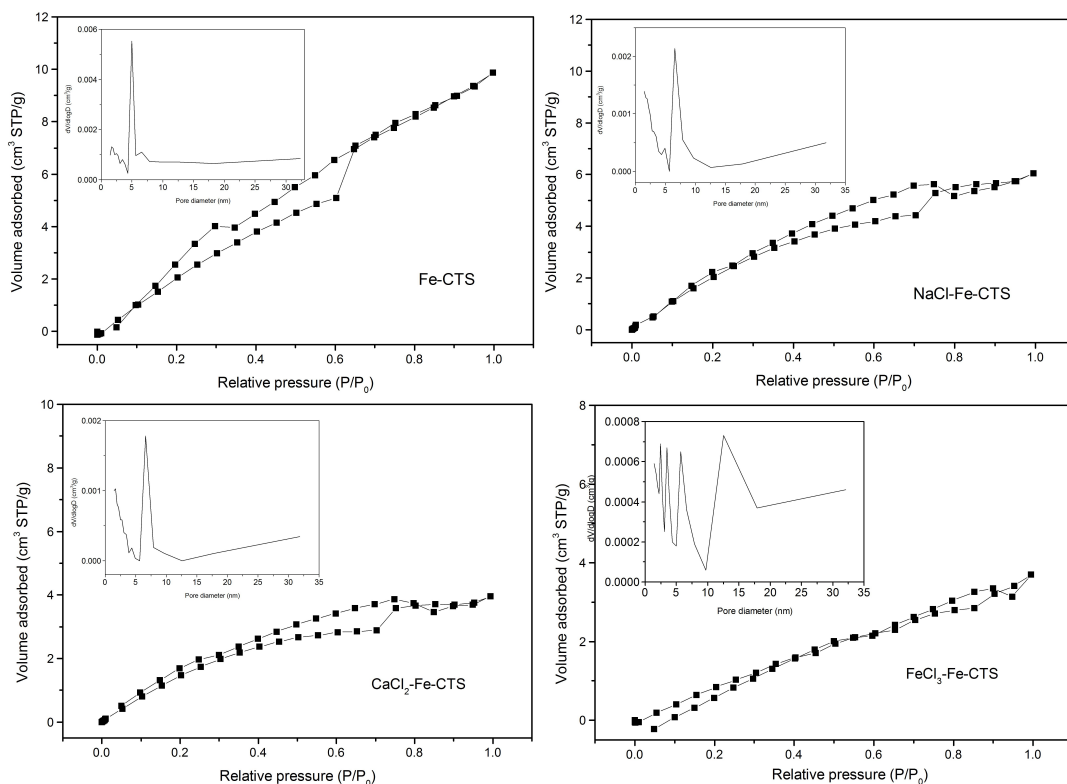


Fig. 5. Nitrogen adsorption-desorption isotherm and pore-size distribution curve of Fe-CTS, NaCl-Fe-CTS, CaCl_2 -Fe-CTS and FeCl_3 -Fe-CTS.

mesopores. [25]. H₃-type hysteresis loops were observed in all the adsorbents, which was related to the adsorbents with aggregates of plate-like particles giving rise to slit-shaped pores [26]. In addition, the hysteresis loop of Fe-CTS shifted to a relatively higher pressure after regeneration, which may be attributed to the increase in pore width [27]. It was found from the figures of pore size distribution that the range of pore size widened after regeneration, especially in FeCl_3 -Fe-CTS. Average pore diameter of Fe-CTS is 4.689 nm, which would be smaller after fluoride adsorption. However, average pore diameter of FeCl_3 -Fe-CTS is 4.691 nm, similar to that of fresh Fe-CTS, indicating that pore diameter widened after spent Fe-CTS was regenerated by FeCl_3 solution. Although the total pore volume of FeCl_3 -Fe-CTS ($0.0057 \text{ cm}^3/\text{g}$) is smaller than that of fresh Fe-CTS ($0.0153 \text{ cm}^3/\text{g}$), fluoride adsorption capacities of these two are almost equal, revealing that ferric ions loaded on spent Fe-CTS have big affinity to fluoride ions. As the radius of F (1.33 \AA) is much smaller than the pore sizes in FeCl_3 -Fe-CTS, F could be transported into the inner of FeCl_3 -Fe-CTS.

FTIR spectra of FeCl_3 -Fe-CTS and spent FeCl_3 -Fe-CTS are shown in Fig. S2. The

peaks between 3600-3200 cm^{-1} were ascribed to intermolecular hydrogen bonds and the overlap between O-H and N-H stretching vibration [28, 29]. The characteristic peaks centered at 1636, 1542, and 1402 cm^{-1} were assigned to N-H deformation, amide H-N-H deformation, and C-N stretching vibrations, respectively [13]. In addition, the broad bands at 1072 and 500-800 cm^{-1} represented vibration C-O and Fe-O bonds in the coordinated complexes, respectively [30, 31]. It is clear that no significant difference were observed between FeCl₃-Fe-CTS and spent FeCl₃-Fe-CTS, demonstrating that no significant structural changes occurred in FeCl₃-Fe-CTS before and after fluoride adsorption.

The XRD patterns of Fe-CTS, FeCl₃-Fe-CTS, CaCl₂-Fe-CTS, and NaCl-Fe-CTS are presented in Fig. S3. The crystalline peaks of Fe-CTS were not observed, demonstrating that Fe-CTS exhibited amorphous nature. It is similar to that observed for granular chitosan-Fe³⁺ complex and Ti-Al binary metal oxide supported chitosan beads [13, 28]. In addition, there were no peaks were observed for FeCl₃-Fe-CTS, CaCl₂-Fe-CTS, and NaCl-Fe-CTS revealing that all these adsorbents were amorphous nature. It may be attributed to the fact that Fe³⁺, Ca²⁺ and Na⁺ were loaded on amorphous Fe-CTS through electrostatic attraction, instead of FeCl₃, CaCl₂, and NaCl crystals covering on the surface of spent Fe-CTS.

Determined on the basis of EDS intensities and relative surface and cross-section compositions of FeCl₃-Fe-CTS before and after adsorption expressed quantitatively as weight percentage are listed in Table 1. Samples 1–8 were obtained from FeCl₃-Fe-CTS before adsorption, while Samples 9–16 were obtained from FeCl₃-Fe-CTS after adsorption. It should be noted that Samples 1–3 and 9–11 were random points from the surface of the beads, and Samples 4–8 and 12–16 were consecutive points obtained along the radius of FeCl₃-Fe-CTS before and after adsorption from the outside to the inside on the cross-section of the beads. It was found that the weight percentage of fluoride on the surface of the beads after regeneration was low. However, the weight percentage of fluoride rapidly increased from an average value of 1.36% FeCl₃-Fe-CTS before adsorption to an average value of 8.03% after adsorption. This result indicated that fluoride had adsorbed on the

adsorbent. It was also found that the amount of fluoride tended to decrease with the distance between the point and the spherical centre, which indicated that internal diffusion occurred in the fluoride adsorption process. This phenomenon became more apparent on FeCl₃-Fe-CTS after adsorption. For Samples 12–16, there was a decline in the weight percentage from 8.654% to 0.498%. More than twice the weight of fluoride was detected on the cross-section of FeCl₃-Fe-CTS after adsorption than before adsorption, suggesting that the regeneration accelerated the rate of internal diffusion. It was also observed that the weight percentage of chloride ranged from an average value of 1.97% before adsorption to an average value of 0.52% after adsorption.

Table 1 EDS results for regenerated Fe-CTS
Table. 1 Results of EDS of regenerated Fe-CTS

	Samples	F (wt%)	Cl (wt%)	Samples	F (wt%)	Cl (wt%)
Surface	1	0.248	1.453	9	5.507	0.471
	2	3.462	3.250	10	7.728	0.258
	3	0.359	1.207	11	10.868	0.824
Cross section	Samples	4	5	6	7	8
	F (wt%)	1.145	0.619	0.623	0.598	0.521
	Samples	12	13	14	15	16
	F (wt%)	8.654	5.458	3.993	2.596	0.498

pHpzc is the pH at which the surface charge, surface potential and ξ -potential are zero. If the solution pH < pHpzc, the adsorbent surface is positively charged, otherwise the surface is negatively charged [32]. The pHpzc value of the Fe-CTS was determined as 4.92 using a pH drift method [33]. The pH of the solution after fluoride adsorption was 5.24, illustrating that the spent Fe-CTS was negatively charged. Table 2 showed that the pH of all FeCl₃ solutions after regenerating spent Fe-CTS was less than 4.92, indicating that FeCl₃-Fe-CTS was positively charged. The surface charge density or surface potential (E in volts) can be simply related to the pH and the Nernst equation Eq. (3.1) [34] and can be written as Eq. (3.2) [35]:

$$E = E_0 + R_g T \ln a_i / n_i F \quad (2)$$

$$E = 2.303R_gT[(p.z.c.) - \text{pH}] / F \quad (3)$$

where E_0 is the standard electrode potential when the concentration of ions is unity, n_i is the valence state of ions, a_i is the activity of ions, R_g is the gas constant, T is temperature and F is the Faraday's constant.

At room temperature, Eq. (3.2) can be further simplified as Eq. (3.3) [35]:

$$E \approx 0.06[(p.z.c.) - \text{pH}] \quad (3.3)$$

Thus, the pH of FeCl_3 regenerants appeared to decrease from 3.50 to 2.92 with increasing concentration, suggesting that the higher the concentration of FeCl_3 regenerants, the higher the positive charge on $\text{FeCl}_3\text{-Fe-CTS}$. Accordingly, it was sufficient to ensure that the Fe-CTS regenerated by 150 mg/L Fe^{3+} with the lowest pH possessed the largest positive charge, which was consistent with the result that it attained the highest fluoride adsorption capacity of 14.44 mg/g.

Table 2 pH of FeCl_3 solution after regeneration

Concentration of Fe^{3+} (mg/L)	30	60	90	120	150
pH	3.50	3.14	3.02	2.94	2.92

To examine the stability of $\text{FeCl}_3\text{-Fe-CTS}$, Fe^{3+} leaching was observed in the fluoride solution after adsorption. Under the experimental conditions, only 0.0661 mg/L of total iron was leached from $\text{FeCl}_3\text{-Fe-CTS}$ into the surrounding solution, indicating that $\text{FeCl}_3\text{-Fe-CTS}$ could be safely used for the removal of fluoride.

3.4 Regeneration and fluoride adsorption mechanisms

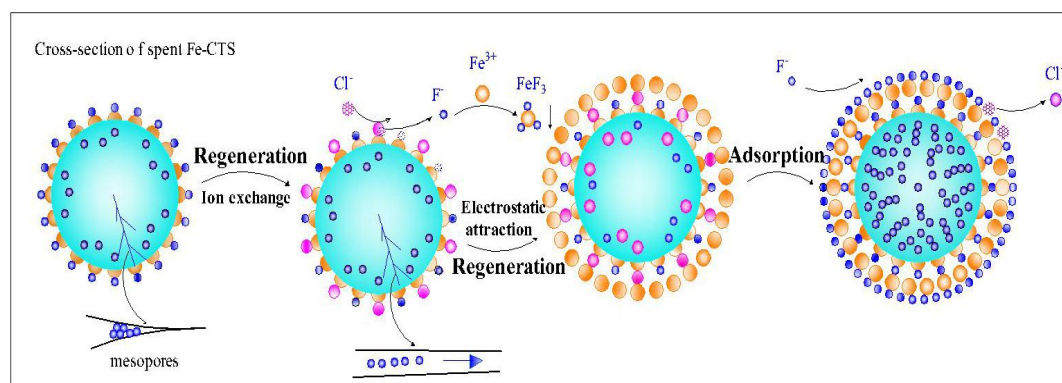


Fig. 6. Possible regeneration/adsorption mechanisms of spent Fe-CTS .

The multiple experimental results and techniques used here together with the surface charge distribution provided valuable information regarding the regeneration of spent Fe-CTS by FeCl_3 . The SEM images identified morphology changes, i.e. holes and cracks emerged. These changes in morphology may lead to the internal diffusion of fluoride. Furthermore, the EDS detected a significant distribution of fluoride on the cross-section of the adsorbent, i.e. fluoride decreased from the outside toward the spherical centre, which indicated that internal diffusion had accelerated. The pH of the FeCl_3 solutions used to regenerate spent Fe-CTS was less than 4.92, indicating that FeCl_3 -Fe-CTS was positively charged, which could attract the negatively charged fluoride ions. On one hand, the positively charged adsorbent could attract much more fluoride onto the surface of the adsorbent, allowing more fluoride to be adsorbed by chemisorption. On the other hand, more fluoride was adsorbed by electrostatic attraction on the surface of regenerated Fe-CTS. Consequently, the fluoride adsorption capacity was enhanced. Moreover, with a similar trend observed for fluoride and chloride, it was assumed that the strongly adsorbed fluoride ions may actually displace the weakly adsorbed chloride ions through ion exchange, which had been validated by extended X-ray absorption fine-structure spectroscopy in the previous study [14]. The displacement of weakly adsorbed chloride ions was also confirmed by the EDS results that showed that as fluoride adsorbed onto the adsorbent, the weight percentage of chloride decreased. It should be noted that the changes in concentration of fluoride were to some extent, all larger than that of chloride, indicating that other mechanisms, such as electrostatic attraction, contributed to fluoride adsorption.

All evidence presented in this study shed light on the importance of potential mechanisms responsible for spent Fe-CTS regeneration (Fig. 6). First, a small amount of fluoride ions was exchanged with chloride ions during regeneration, increasing the adsorption sites for fluoride. In addition, the fluoride ions exchanged with chloride ions may form a precipitate with iron ions. Furthermore, iron ions were attracted to the negatively charged spent Fe-CTS through electrostatic attraction, which resulted in a positively charged regenerated adsorbent. Subsequently, the fluoride that reached the surface of the adsorbent diffused into the interior of the adsorbent through the

mesopores. In turn, the conditions for negatively charged fluorine ions are more favourable. Eventually, ion exchange occurred between the chloride and fluoride ions, and the fluoride ions were adsorbed and diffused to the interior of the adsorbent. A small portion of the fluoride ions were electrostatically attracted to the surface of the adsorbent.

3.5 Continuous regeneration/adsorption cycles

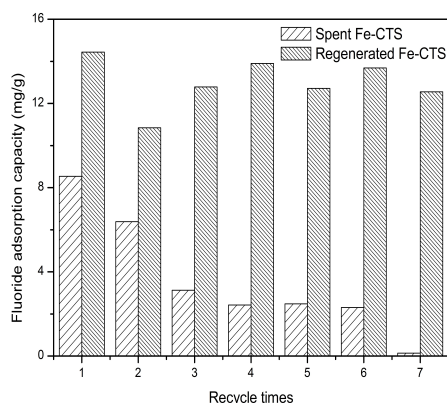


Fig.7. Adsorption capacity of continuous adsorption/regeneration cycles.

Regeneration experiments were performed to determine the reusability of fluoride adsorption and industrial availability [36]. The adsorption/regeneration cycles, which started with spent Fe-CTS, were repeated seven times for the same batch of adsorbent. Although with limited desorption, the superiority of regeneration using 150 mg/L Fe^{3+} solution was confirmed by comparing the adsorption capacity of the spent adsorbent without regeneration, as shown in Fig. 7. It was found that fluoride adsorption onto Fe-CTS was significantly enhanced after every regeneration cycle. The adsorption capacity of spent Fe-CTS gradually decreased with increasing adsorption cycles. This trend had also been observed for other chitosan-based adsorbents [13, 37-39] and had been attributed to the increasing adsorbate molecules that were strongly attached to the surface of adsorbents, possibly via chemical adsorption [40]. The adsorption capacity of spent Fe-CTS without regeneration declined dramatically and was close to zero in the seventh cycle, which may indicate that fluoride adsorption on Fe-CTS had reached saturation. The maximum adsorption capacity of Fe-CTS was 40.37 mg/g higher than that of neodymium-modified chitosan (22.38 mg/g) [10], chitosan supported lanthanum (III) and zirconium (IV) mixed oxides beads (29.76 mg/g) [41],

and aluminium and doping chitosan-Fe(III) hydrogel (Al-CS-Fe, 31.16 mg/g) [11]. It was obvious that the adsorption capacity of regenerated Fe-CTS was much higher than that of spent Fe-CTS for the same cycles. Slight fluctuations were observed in the adsorption capacity of regenerated Fe-CTS for seven cycles, and the adsorption capacity was approximately 13 mg/g. The total adsorption capacity of Fe-CTS regenerated for seven cycles was 74.04 mg/g, excluding the amount of fluoride desorbed in regeneration. These results indicated that FeCl_3 solution was a promising regenerant for Fe-CTS.

4. Conclusion

In this study, FeCl_3 as a regenerant yielded much higher regeneration efficiency than NaCl and CaCl_2 . A 150 mg/L Fe^{3+} solution showed great regeneration efficiency; a fluoride adsorption capacity of 14.44 mg/g approximated the adsorption capacity of fresh Fe-CTS (14.99 mg/g). The results obtained from SEM images and the EDS indicated that the regeneration using FeCl_3 accelerated the internal diffusion of fluoride by increasing and broadening the mesopores. The Fe-CTS regenerated by 150 mg/L Fe^{3+} with the lowest pH, i.e. 2.92, which was smaller than pH_{pzc} 4.92, showed the highest positive charge. The EDS results for the change in the concentration of fluoride and chloride ions showed that the weight percentage of chloride decreased with fluoride adsorption onto the adsorbent and confirmed that ion exchange was a major mechanism in the adsorption process. The amount of fluoride adsorbed on Fe-CTS was greater than the amount of chloride exchanged with fluoride from the Fe-CTS, suggesting that another mechanism such as electrostatic attraction existed. The total adsorption capacity of FeCl_3 -Fe-CTS was 74.04 mg/g for seven regeneration/adsorption cycles without a significant loss in the adsorption ability and only 0.0661 mg/L of total iron from regenerated Fe-CTS was leached into the surrounding solution. These results indicated that regenerating spent Fe-CTS using FeCl_3 would be a safe and practical method.

Acknowledgments

The authors thank the National Natural Science Foundation of China (NSFC) (No. 21407129), the “Beijing National Science Foundation (8144053)” and the “Fundamental Research Funds for the Central Universities (2652015240)” for financial support for this work.

References

- [1] J. He, J.P. Chen, A zirconium-based nanoparticle: Essential factors for sustainable application in treatment of fluoride containing water, *Journal of Colloid and Interface Science*, 416 (2014) 227–234.
- [2] K.D. Brahman, T.G.Kazi, H.I. Afridi, S. Naseem, S.S. Arain, N. Ullah, Evaluation of high levels of fluoride, arsenic species and other physicochemical parameters in underground water of two sub districts of Tharparkar, Pakistan: A multivariate study, *Water Research*, 47 (2013) 1005–1020.
- [3] L. Chai, Y. Wang, N. Zhao, W. Yang, X. You, Sulfate-doped $\text{Fe}_3\text{O}_4/\text{Al}_2\text{O}_3$ nanoparticles as a novel adsorbent for fluoride removal from drinking water, *Water Research*, 47 (2013) 4040-4049.
- [4] S.W. Nahm, W.G. Shim, Y.-K. Park, S.C. Kim, Thermal and chemical regeneration of spent activated carbon and its adsorption property for toluene, *Chemical Engineering Journal*, 210 (2012) 500-509.
- [5] K. Biswas, K. Gupta, U.C. Ghosh, Adsorption of fluoride by hydrous iron(III)-tin(IV) bimetal mixed oxide from the aqueous solutions, *Chemical Engineering Journal*, 149 (2009) 196-206.
- [6] L. Feng, W. Xu, T. Liu, J. Liu, Heat regeneration of hydroxyapatite/attapulgite composite beads for defluoridation of drinking water, *Journal of Hazardous Materials*, 221 (2012) 228-235.
- [7] H. Lounici, L. Adour, D. Belhocine, A. Elmidaoui, B. Bariou, N. Mameri, Novel technique to regenerate activated alumina bed saturated by fluoride ions, *Chemical Engineering Journal*, 81 (2001) 153-160.
- [8] K. Sasaki, N. Fukumoto, S. Moriyama, Q. Yu, T. Hirajima, Chemical regeneration of magnesium oxide used as a sorbent for fluoride, *Separation and Purification Technology*, 98 (2012) 24-30.

- [9] P. Liao, S. Yuan, W. Xie, W. Zhang, M. Tong, K. Wang, Adsorption of nitrogen-heterocyclic compounds on bamboo charcoal: Kinetics, thermodynamics, and microwave regeneration, *Journal of Colloid and Interface Science*, 390 (2013) 189-195.
- [10] R. Yao, F. Meng, L. Zhang, D. Ma, M. Wang, Defluoridation of water using neodymium-modified chitosan, *Journal of Hazardous Materials*, 165 (2009) 454-460.
- [11] J. Ma, Y. Shen, C. Shen, Y. Wen, W. Liu, Al-doping chitosan-Fe(III) hydrogel for the removal of fluoride from aqueous solutions, *Chemical Engineering Journal*, 248 (2014) 98-106.
- [12] S. Jagtap, M.K. Yenkie, S. Das, S. Rayalu, Synthesis and characterization of lanthanum impregnated chitosan flakes for fluoride removal in water, *Desalination*, 273 (2011) 267-275.
- [13] D. Thakre, S. Jagtap, N. Sakhare, N. Labhsetwar, S. Meshram, S. Rayalu, Chitosan based mesoporous Ti-Al binary metal oxide supported beads for defluoridation of water, *Chemical Engineering Journal*, 158 (2010) 315-324.
- [14] J. Zhang, N. Chen, Z. Tang, Y. Yu, Q.L. Hu, C.P. Feng, A study of the mechanism of fluoride adsorption from aqueous solutions onto Fe-impregnated chitosan, *Physical Chemistry Chemical Physics*, 17 (2015) 12041-12050.
- [15] P. Baskaralingam, M. Pulikesi, D. Elango, V. Ramamurthi, S. Sivanesan, Adsorption of acid dye onto organobentonite, *Journal of Hazardous Materials*, 128 (2006) 138-144.
- [16] L. Halla Velazquez-Jimenez, R.H. Hurt, J. Matos, J. Rene Rangel-Mendez, Zirconium-Carbon Hybrid Sorbent for Removal of Fluoride from Water: Oxalic Acid Mediated Zr(IV) Assembly and Adsorption Mechanism, *Environmental Science & Technology*, 48 (2014) 1166-1174.
- [17] M.L. Jimenez-Nunez, M. Solache-Rios, J. Chavez-Garduno, M.T. Olguin-Gutierrez, Effect of grain size and interfering anion species on the removal of fluoride by hydrotalcite-like compounds, *Chemical Engineering Journal*, 181 (2012) 371-375.
- [18] A. Aziz, M. Sajjad, B. Mohammad, Elemental characterization of black shales of Khyber Pakthunkhawa (KPK) region of Pakistan using AAS, *Chinese Journal of Geochemistry*, 32 (2013) 248-251.
- [19] B.X. Peng, D.S. Wu, J.H. Lai, H.Y. Xiao, P. Li, Simultaneous determination of halogens (F, Cl, Br, and I) in coal using pyrohydrolysis combined with ion chromatography, *Fuel*, 94 (2012) 629-631.

- [20] C.S. Shen, Y. Shen, Y.Z. Wen, H.Y. Wang, W.P. Liu, Fast and highly efficient removal of dyes under alkaline conditions using magnetic chitosan-Fe(III) hydrogel, *Water Research*, 45 (2011) 5200-5210.
- [21] J.E. Jorgensen, J.S. Olsen, L. Gerward, Compression mechanism of GaF₃ and FeF₃: a high-pressure X-ray diffraction study, *High Pressure Research*, 30 (2010) 634-642.
- [22] W.D. Tian, Y.Q. Ma, Molecular Dynamics Simulations of a Charged Dendrimer in Multivalent Salt Solution, *Journal of Physical Chemistry B*, 113 (2009) 13161-13170.
- [23] W. Xiang, G. Zhang, Y. Zhang, D. Tang, J. Wang, Synthesis and characterization of cotton-like Ca-Al-La composite as an adsorbent for fluoride removal, *Chemical Engineering Journal*, 250 (2014) 423-430.
- [24] Y. Han, X. Quan, S. Chen, S. Wang, Y. Zhang, Electrochemical enhancement of adsorption capacity of activated carbon fibers and their surface physicochemical characterizations, *Electrochimica Acta*, 52 (2007) 3075-3081.
- [25] K. S. W. Sing, D. H. Everett, R. A. W. Haul, Reporting physisorption data for gas/solid systems with special reference to the determination of surface area and porosity (Recommendations 1984), *Pure & Appl. Chem.*, 57 (1985) 603-619.
- [26] J. Rouquerol, D. Avnir, C. W. Fairbridge, D. H. Everett, J. H. Haynes, N. Pernicone, J. D. F. Ramsay, K. S. W. Sing and K. K. Unger, recommendations for the characterization of porous solids, *Pure & Appl. Chem.*, 66 (1994) 1739-1758.
- [27] Y. H. Zeng, P. Phadungbut, D. D. Do and D. Nicholson, Anatomy of Adsorption in Open-End and Closed-End Slit Mesopores: Adsorption, Desorption, and Equilibrium Branches of Hysteresis Loop, *J. Phys. Chem. C*, 118 (2014), 25496–25504.
- [28] Q. L. Hu, N. Chen, C.P. Feng, and W.W. Hu, Nitrate adsorption from aqueous solution using granular chitosan-Fe³⁺ complex, *Applied Surface Science*, 347 (2015) 1–9.
- [29] S. Biniak, G. Szymanski, J. Siedlewski and A. Swiatkowski, the characterization of activated carbons with oxygen and nitrogen surface groups, *Carbon*, 35 (1997) 1799-1810.
- [30] L. H. V. Jimenez, R. H. Hurt, J. Matos and J. R. R. Mendez, Zirconium–Carbon Hybrid Sorbent for Removal of Fluoride from Water: Oxalic Acid Mediated Zr(IV) Assembly and Adsorption Mechanism, *Environmental Science and Technology*, 48 (2014) 1166–1174.
- [31] L. Batistella, L.D. Venquiaruto, M.D. Luccio, J.V. Oliveira, S.B.C. Pergher, M.A. Mazutti, D.

de Oliveira, A.J. Mossi, H. Treichel, R.Dallago, Evaluation of Acid Activation under the Adsorption Capacity of Double Layered Hydroxides of Mg-Al-CO₃ Type for Fluoride Removal from Aqueous Medium, *Industrial and Engineering Chemistry Research*, 50 (2011) 6871–6876.

[32] J.M. Wang, X.J. Teng, H. Wang, H. Ban, Characterizing the metal adsorption capability of a class F coal fly ash, *Environmental Science & Technology*, 38 (2004) 6710-6715.

[33] T. Lv, W. Ma, G. Xin, R. Wang, J. Xu, D. Liu, F. Liu, D. Pan, Physicochemical characterization and sorption behavior of Mg-Ca-Al (NO₃) hydrotalcite-like compounds toward removal of fluoride from protein solutions, *Journal of Hazardous Materials*, 237 (2012) 121-132.

[34] A.C. Pierre, *Introduction to sol-gel processing*[M]. Kluwer Academic Publishers, 1998.

[35] G.Z. Cao, Y. Wang, *Nanostructures and nanomaterials: synthesis, properties, and application*[M]. World Scientific Publishing Co. Pte. Ltd, 2011.

[36] T. Wang, K. Kailasam, P. Xiao, G. Chen, L. Chen, L. Wang, J. Li, J. Zhu, Adsorption removal of organic dyes on covalent triazine framework (CTF), *Microporous and Mesoporous Materials*, 187 (2014) 63-70.

[37] S.K. Swain, T. Padhi, T. Patnaik, R.K. Patel, U. Jha, R.K. Dey, Kinetics and thermodynamics of fluoride removal using cerium-impregnated chitosan, *Desalination and Water Treatment*, 13 (2010) 369-381.

[38] S.K. Swain, R.K. Dey, M. Islam, R.K. Patel, U. Jha, T. Patnaik, C. Airoidi, Removal of Fluoride from Aqueous Solution Using Aluminum-Impregnated Chitosan Biopolymer, *Separation Science and Technology*, 44 (2009) 2096-2116.

[39] Y. Zhang, Y. Xu, H. Cui, B. Liu, X. Gao, D. Wang, P. Liang, La(III)-loaded bentonite/chitosan beads for defluoridation from aqueous solution, *Journal of Rare Earths*, 32 (2014) 458-466.

[40] M. Auta, B.H. Hameed, Chitosan-clay composite as highly effective and low-cost adsorbent for batch and fixed-bed adsorption of methylene blue, *Chemical Engineering Journal*, 237 (2014) 352-361.

[41] S.M. Prabhu, S. Meenakshi, Enriched fluoride sorption using chitosan supported mixed metal oxides beads: Synthesis, characterization and mechanism, *Journal of Water Process Engineering*, 2 (2014) 96-104.